Neutron vibrational spectroscopy and first-principles calculations of the ternary hydrides $Li_4Si_2H(D)$ and $Li_4Ge_2H(D)$: Electronic structure and lattice dynamics

Hui Wu,[1,2,*] Wei Zhou,[1,3] Terrence J. Udovic,[1] John J. Rush,[1,2] Taner Yildirim,[1,3] Michael R. Hartman,[4] Robert C. Bowman, Jr.,[5] and John J. Vajo[6]

[1]*NIST Center for Neutron Research, National Institute of Standards and Technology, 100 Bureau Drive, MS 6102, Gaithersburg, Maryland 20899-6102, USA*

[2]*Department of Materials Science and Engineering, University of Maryland, College Park, Maryland 20742-2115, USA*

[3]*Department of Materials Science and Engineering, University of Pennsylvania, 3231 Walnut Street, Philadelphia, Pennsylvania 19104-6272, USA*

[4]*Department of Nuclear Engineering and Radiation Health Physics, Oregon State University, 116 Radiation Center, Corvallis, Oregon 97331-5903, USA*

[5]*Jet Propulsion Laboratory, California Institute of Technology, Pasadena, California 91109-8099, USA*

[6]*HRL Laboratories, LLC, Malibu, California 90265, USA*

(Received 21 May 2007; revised manuscript received 7 August 2007; published 17 December 2007)

Using combined neutron spectroscopy and first-principles calculations, we investigated the electronic structure and vibrational dynamics of the recently discovered class of ternary hydrides Li_4Tt_2H (Tt=Si and Ge). In these compounds, all hydrogen atoms are located in a single type of Li_6-defined octahedral site. The Tt atoms form long-range Tt-Tt chains sandwiched between each Li_6-octahedra layer. The Li-H interactions are strongly ionic, with bond lengths comparable to those in LiH. Our density functional theory calculations indicate that Li atoms transfer their electrons to both H and Tt atoms. Tt atoms within the Tt-Tt chain are bonded covalently. The electronic density of states reveals that both hydrides exhibit metallic behavior. The observed vibrational spectra of these hydrides are in good overall agreement with the calculated phonon modes. There is evidence of dispersion induced splitting in the optical phonon peaks that can be ascribed to the coupling of H vibrations within the Li_6-octahedra layers.

DOI: 10.1103/PhysRevB.76.224301 PACS number(s): 63.20.Dj, 71.20.−b, 71.15.Mb, 78.70.Nx

I. INTRODUCTION

The Li-Si and Li-Ge binary phase diagrams have been well established.[1–4] Most of these phases show quite strong thermal stability and interesting structural diversity. Due to the relatively large cohesive energies of these lithium silicide and germanide phases, it was found that the strongly bound H atoms in LiH could be effectively destabilized by the addition of Si (Refs. 5 and 6) or Ge.[7] Consequently, the Si or Ge-doped LiH (~12.5 wt % H) dehydrogenates at a much lower temperature via the formation of various Li-Si or Li-Ge alloy phases concomitant with H_2 release.

Interestingly, during dehydrogenation/hydrogenation studies of LiH/Si and LiH/Ge mixtures, two new isostructural, ternary hydride phases, Li_4Si_2H and Li_4Ge_2H, were formed.[7] To the best of our knowledge, H insertion into lithium silicides and germanides has not been reported previously. Thus, in contrast to the rich phase diagrams of Li-Si(Ge) binary systems, Li_4Si_2H and Li_4Ge_2H are the first and the only known compounds in the Li-Si(Ge)-H ternary systems.

We have recently reported the structure of these two hydride phases.[7] Figure 1 shows the refined crystal structure (*Cmmm*, No. 65) of Li_4Ge_2H and Li_4Si_2H. In these compounds, hydrogen atoms are located in the interstitial octahedral ($2d$) sites exclusively defined by Li cations. These Li_6 octahedra share corners with four other in-plane neighboring octahedra, forming Li_6-octahedral layers at h and $h/2$ ($h=0,1,2,\ldots,n$) planes. All Li_6 octahedra are identical, with three pairs of Li–H bonds along the **a**, **b**, and **c** directions, respectively. Thus, there is only one crystallographic site for interstitial hydrogen atoms. Such a Li_6-octahedral site is unique; in fact, it is so far the only reported octahedral interstitial site confined by single type of alkali metal in all known ternary hydride phases. Between two Li_6-octahedral layers, Ge or Si atoms align in a zigzag fashion, propagating

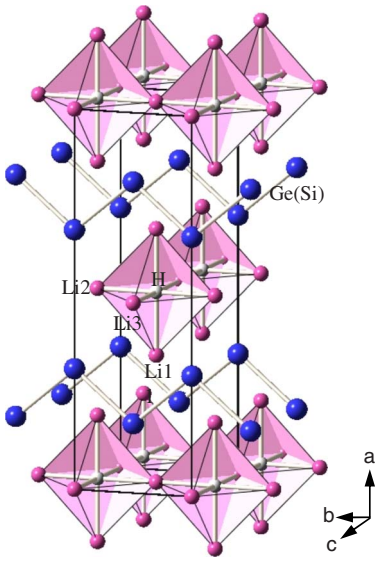

FIG. 1. (Color online) An off-[001] view of the orthorhombic Li_4Tt_2H crystal structure with centered octahedral interstices. The large blue and small pink spheres represent Tt (=Si, Ge) and Li, respectively, and the interstitial H atoms (small white) are centered in the shaded Li_6 octahedra

along the **b** direction in the **c** basal planes. The Ge–Ge and Si–Si bond distances in these long-range *–Tt–Tt–* chains are much longer than the isolated *Tt-Tt* dimers in the binary Li-*Tt* (*Tt*=Si and Ge) intermetallics, but comparable to those of the dimers in Ca_5Tt_3 and $Ca_5Tt_3H_x$, and to those similarly bonded clathrate II network structures $A_8A'_{16}Tt_{136}$ (*A*, *A'*=alkali metals, *Tt*=Si and Ge).[8]

The discovery of Li_4Si_2H and Li_4Ge_2H is a significant advance in our understanding of the Li-Si-H and Li-Ge-H ternary phase diagrams, which up to this point were in error. In addition to determining the structure, a thorough study of the interatomic bonding and stability of these previously unknown hydrides is necessary for a better understanding of their properties. A study of the hydrogen site is of particular interest to researchers dealing with the destabilization of the light-metal hydrides. In this paper, we present the results of neutron vibrational spectroscopy (NVS) and first-principles calculations on these ternary hydrides to better reveal the nature of their bonding interactions and the origin of their stabilities. Such information should contribute to a better overall understanding of hydride destabilization in LiH and similar light-metal hydride systems. The calculated electronic structures should also be useful for any potential applications involving their physical properties.

II. MATERIALS AND EXPERIMENTAL METHODS

The Li_4Ge_2H and Li_4Ge_2D powder samples were synthesized via the following procedures. First, a 2:1 LiH (Alfa Aesar[9] 99.4%) and Ge (Alfa Aesar 99.999%) stoichiometric mixture was ball-milled with a Fritsch Pulverisette 7 planetary mill at 400 rpm for 30 min. The mixture was then heated and evacuated at 763 K in dynamic vacuum for 8–10 h to expel H_2. The products were then reground with an agate mortar and pestle in a He-filled glovebox. Finally, the hydrided or deuterided samples were prepared by direct reaction of the alloy with gas-phase H_2 or D_2 (99.999%) at 723–743 K under 2.5 MPa pressure. The compositions and structures of the products after each synthesis process were characterized using laboratory x-ray diffraction (Rigaku, D-MAX/UltimaIII) and neutron prompt-gamma activation analysis (PGAA) techniques.[10] Powders were wrapped in a Mo envelope and sealed in a stainless-steel tube during the high-temperature hydrogenation. All sample handling was performed in a He-filled glovebox to avoid oxidation reactions. The stoichiometry of the resultant Li_4Ge_2H sample was verified by PGAA. The deuterium content of the isostructured Li_4Ge_2D sample was confirmed gravimetrically.

The Li_4Si_2H and Li_4Si_2D powder samples were prepared using a modified procedure to maximize their formation. First, a LiH (Fluka, 97%)+Si (cleaved from electronic grade wafers) 1:1 stoichiometric mixture was ball milled (400 rpm for 1 h, see Ref. 6 for details) then evacuated at 773 K for 2–3 h to remove the hydrogen. Next, the LiSi alloy mixture was hydrided or deuterided to a stoichiometry of LiSiH or LiSiD with ≈0.7 MPa of H_2 or D_2 (99.999%) at 723 K. Again, hydrogen content was verified by PGAA. Finally, a portion of the H or D was removed from the sample to a final ratio of 0.25 H(D)/Li by controlled evacuation at 723 K followed by annealing for 8–9 d at 723 K in a sealed stainless-steel sample tube. The final sample composition was approximately $Li_4Si_2H(D)+2Si$. The presence of excess Si was found to be necessary to promote $Li_4Si_2H(D)$ formation instead of LiH(D).

The NVS measurements were performed at the NIST Center for Neutron Research (NCNR) using the BT-4 Filter-Analyzer Neutron Spectrometer[11] with the Cu(220) monochromator under conditions that provided full-width-at-half-maximum energy resolutions of 2–4.5% of the incident energy over the range probed. PGAA measurements were performed at the NCNR with the NG-6 high-resolution γ-ray spectrometer.

First-principles calculations were performed within the plane-wave implementation of the generalized gradient approximation to density functional theory (DFT) using the PWSCF package.[12] We used a Vanderbilt-type ultrasoft potential with Perdew-Burke-Ernzerhof exchange correlation. A cutoff energy of 480 eV and a $6\times6\times8$ *k*-point mesh were found to be enough for the total energy to converge within 0.5 meV/ atom and 0.005 eV/Å. Structure optimizations were performed with respect to lattice parameters and atomic positions. The phonon calculations were conducted with the optimized structure using the supercell method with finite difference.[13,14]

III. RESULTS AND DISCUSSION

According to our previous neutron-diffraction-based structural results for the deuterided samples,[7] the three different Li–D bond lengths associated with the Li_6 octahedra (i.e., Li1-D, Li2-D, and Li3-D in Fig. 1) were in the range of 1.88–2.09 Å. These values are comparable to that in pure LiH (Li-H ~ 2.031 Å), indicating quite strong Li–H bonding. Also, the nearest Li-*Tt* (*Tt*=Si and Ge) distances are significantly lengthened compared to those in the various Li-Ge and Li-Si intermetallic binaries,[15–19] indicating the weakened interactions between Li and *Tt* atoms. Therefore, as we previously proposed, it is the strong Li–H bonding that likely stabilizes these ternary hydride phases. In order to better understand the bonding nature and local bonding configuration, we performed first-principles DFT calculations on these phases. We first optimized the *Cmmm* crystal structures. The relaxed atomic positions agreed well with our refined values for Li_4Si_2D and Li_4Ge_2D. Figure 2 plots the total electron densities of states (DOSs) and their projections on the different atomic sites for the *Cmmm* structures of Li_4Si_2D and Li_4Ge_2D. Both hydrides show similar electronic band structures. The prominent (≈1–1.5 eV width) low-energy feature observed in the total DOS (centered about 5.2 eV below the Fermi energy, E_F) corresponds to Li–H bands in both hydrides. Only Li 2*s* states participate in the H-metal bonding. Again, consistent with our previous suggestion based on diffraction results,[7] the strong Li-H interaction plays a crucial role in stabilizing these ternary hydrides, due to its lowering of the energy of the Li *s* states below the Fermi level of the hydrides. The total DOS band structure at higher energy is governed by the strong hybridization of Si 3*p* or Ge 4*p* states. The Li 2*s* states are more delocalized, which results in

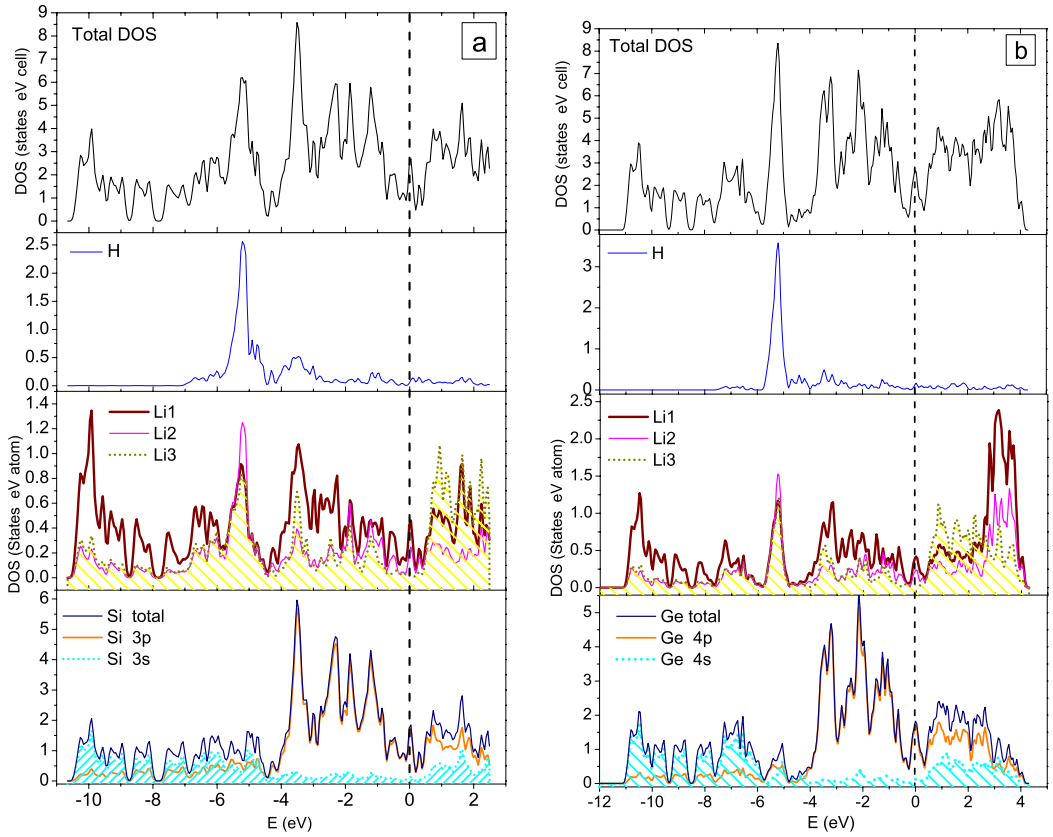

FIG. 2. (Color online) Total electronic DOS of (a) Li_4Si_2H and (b) Li_4Ge_2H and projection around the different atomic sites. E_F is taken as the zero of energy and shown as the dashed line.

much broader bands of lower DOS. The Si $3p$ (Ge $4p$) contributions to DOS at and above E_F are larger than those of the Li s state in both hydrides. Li_4Si_2H and Li_4Ge_2H exhibit metallic behavior due to the finite electron states at the Fermi level $N(E_F)$, which is dominated by the Si $3p$ or Ge $4p$ state. Figure 3 shows five characteristic charge-density maps [i.e., (100) and (002) planes including Li and H, (001) including Li and Si, and (002) and (010) planes including Li, Si, and H]. From Fig. 3, it is clear that electron charge from Li atoms is almost fully transferred to H and Si atoms as there is nearly no electron density left at Li sites. The highest charge density is situated at each H-atom site, indicating very strong H-Li interactions that are primarily ionic. Some charge transfer from Li to Si atoms also indicates an ionic contribution to the bonding between them. The large overlap of the electron clouds between neighboring Si shows strong covalent bonding within the Si-Si chains. This is consistent with the strong hybridization as observed in the DOS (Fig. 2). Therefore, the bonding in Li_4Si_2H and Li_4Ge_2H is a mixture of ionic and covalent characters. The charge densities in the regions between Li, H, and Si chains is rather low, implying the bonding between Li_6-octahedral layers and Si-Si chains is directional but not metallic. Similar charge-density plots were also obtained in Li_4Ge_2H.

To gain additional insight into the nature of bonding in these ternary hydrides, we studied the phonon density of states of these ternary hydrides using neutron vibrational spectroscopy. Figure 4 illustrates the NV spectra of $Li_4Si_2H(D)$ and $Li_4Ge_2H(D)$ at 10 K, respectively. The spectrum for Li_4Si_2H displays three distinct peaks at 84.1, 100.0, and 123.4 meV. Such spectral features are consistent with the refined crystal structure possessing a single H site, since three normal-mode vibrations generally accompany one type of hydrogen site. The deuteride spectrum is similar but downshifted in energy by roughly a factor of $1/\sqrt{2}$ due to the doubled isotopic mass for D compared to H. The spectra of the germanide hydrides are analogous to those of their silicide counterparts, with three main phonon bands at around 86.9, 99.0, and 116.3 meV for Li_4Ge_2H and 61.4, 70.6, and 83.7 meV for Li_4Ge_2D.

To interpret the spectra and correlate the observed phonon density of states with the refined crystal structures, we performed first-principles phonon calculations. The phonon calculations were performed with the optimized structure using the supercell method with finite difference.[14] A cell of $2a\times2b\times2c$ was used and the full dynamical matrix was obtained from a total of 36 symmetry-independent atomic displacements (0.01 Å). The NV spectra of Li_4Ge_2H and Li_4Si_2H were computed for a $10\times10\times10$ q point grid within the incoherent approximation with the instrumental resolution taken into account.[20] The primitive cells of Li_4Si_2H and Li_4Ge_2H contain seven atoms giving rise to a total of 21 phonon branches ($2A_g+2B_{1g}+5B_{1u}+2B_{2g}+5B_{2u}+5B_{3u}$). Inspection of the eigenvectors allows the characterization of the modes. The NV spectrum is dominated by H-atom displacements. Phonon spectra largely associated

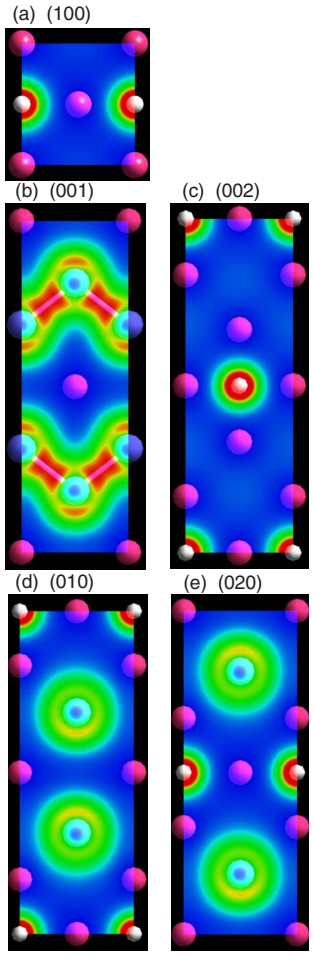

FIG. 3. (Color online) Characteristic charge-density maps on (a) (100), (b) (001), (c) (002), (d) (010), and (e) (020) planes. The values of the contours in all maps are from 0 to 0.57 $e/\text{Å}^2$. The atoms (H, small white; Li, medium pink; Si, large blue spheres) on the corresponding crystallographic planes are also shown underneath the transparent charge-density maps for clarity.

with the metal-atom displacements (peaks between 0 and 30 meV) were not measured. Figure 5 compares the calculated phonon modes with the observed NV spectra. Calculations considering 1-phonon and (1+2)-phonon contributions to NV spectra yield similar spectra in the measured energy range. Three phonon modes in the range of 75–135 meV in the NV spectra of Li_4Si_2H and Li_4Ge_2H originated from H atoms in Li_6-octahedral sites, with increasing phonon-mode energies associated with H vibrations along the different H–Li bond axes with decreasing bond lengths, respectively (i.e., increasing bonding strengths), as expected.

From Fig. 5, the calculated phonon modes for these ternary hydrides agree reasonably well overall with the observed NV spectra. The lowest and highest phonon peaks correspond to the H vibrations along the longest and shortest Li–H bonds within each Li_6 octahedron. Phonon modes at 100.0 meV (Li_4Si_2H) and 99.0 meV (Li_4Ge_2H) originate from the H vibrations along the Li1-H direction. The measured spectra showed some significant weaker sidebands for the lowest and highest vibrational peaks. Since our calculations give single sharp peak while the neutron data show a shoulder on each peak for the hydrogen modes at the Li-octahedral center, it is quite possible that the $2\times2\times2$ supercell used in our calculations is not large enough to capture all possible dispersion of the hydrogen phonon modes. It is also possible that in real materials some of the Li octahedra may have Li vacancy as a defect which could give slightly different phonon modes and show up as a shoulder in the measured spectrum. The middle vibrational peaks in both spectra do not show evidence of dispersion in the phonon branches and can be well reproduced by first-principles calculations. We believe that the indication of dispersion of the phonon modes can be ascribed to the "sandwiched" structure characteristic of these hydride phases. From the crystal structure (Fig. 1), each Li_6 octahedron shares corners (Li2 and Li3) with four neighboring octahedra within the **a** basal planes and leaves the other two vertices (Li1) along the **a** direction unshared. Therefore, vibrations of the H atom in each Li_6 octahedron along the **b** and **c** directions would be more affected by the motions of other H atoms in the neighboring

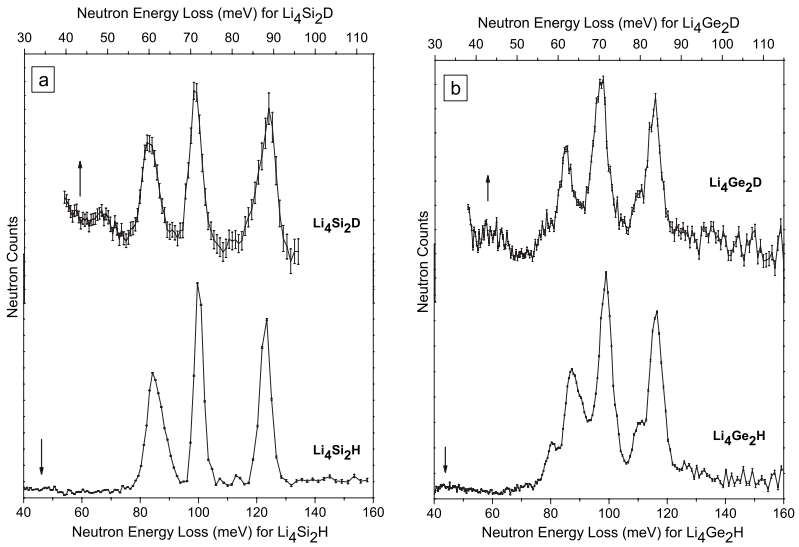

FIG. 4. NV spectra of (a) $Li_4Si_2H(D)$ and (b) $Li_4Ge_2H(D)$ at 10 K. The ratio of corresponding energy-loss scales for hydrides and deuterides is $\sqrt{2}$. The spectra for hydrides and deuterides are plotted using the bottom and the top x axes, respectively.

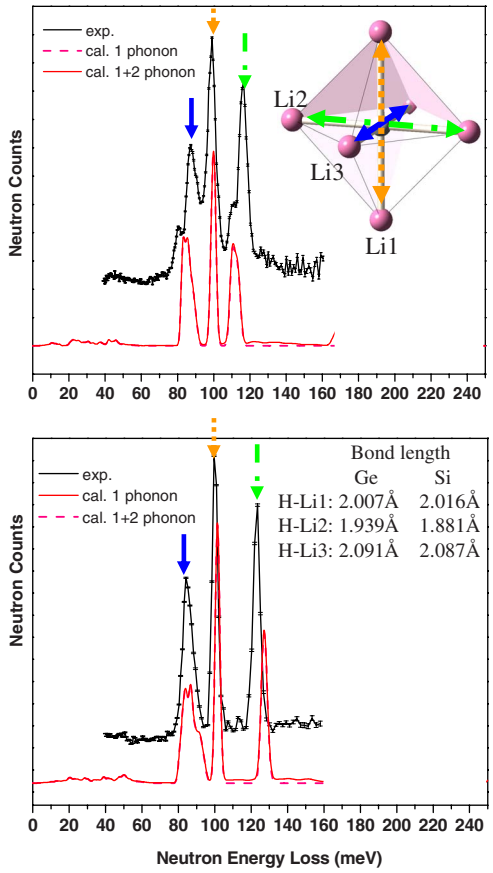

FIG. 5. (Color online) Comparison of observed NV spectra of Li_4Si_2H (bottom panel) and Li_4Ge_2H (top panel) with the calculated spectra. The inset schemes the assigned H phonon modes corresponding to their observed peaks in the NV spectra (solid, dot, and dash-dot arrows indicate the H phonon modes in Li_6-octahedron and the corresponding observed peaks in NV spectra, respectively), which are well correlated with the Li-H bond lengths.

octahedra and most likely couple with these motions. Consequently, the coupling of vibrations along these two directions within the octahedral layers can induce dispersion of the corresponding phonon modes. The vibrations of H atoms along the **a** direction will not be so affected because the octahedral H sites are interrupted by Si-Si or Ge-Ge chains along this direction. As a result, the middle peaks in both spectra are sharp features without evidence of dispersion.

The formation of the Li-Si-H and Li-Ge-H ternaries is surprising as they have not been previously identified in spite of the well-established and rich Li-Si and Li-Ge phase diagrams. Notably, Li_2Si and Li_2Ge, which possess the same Li/Si(Ge) ratios as in the ternary hydrides, are not, by themselves, known stable binary Li-Si(Ge) phases. Thus, it is important to understand why these particular ternary hydride phases can exist and be stable at room temperature. As we have pointed out, these ternaries exhibit an unusual structure with a unique Li_6-octahedral hydrogen site and long-range Si-Si (and Ge-Ge) two-dimensional chains.

Our electronic structure study reveals a strong ionic bonding between Li and H, which is primarily responsible for the stabilization and existence of these ternaries, in contrast to the lack of "Li_2Si" and "Li_2Ge" phases in prior literature. Our results do not necessarily indicate that these ternaries are more stable than the known Li_xSi_y or Li_xGe_y binaries. Yet, the recognition of these ternary hydrides certainly advances our understanding of the current Li-Si-H and Li-Ge-H phase diagrams, and more importantly, the mechanism and the reaction path of hydride destabilization in these and perhaps other alloy hydrides.

IV. SUMMARY

Using combined neutron vibrational spectroscopy and first-principles calculations, we investigated the electronic structure and lattice dynamics of a new class of ternary hydrides Li_4Tt_2H (Tt=Si and Ge). Our calculations confirmed that the formation of these new ternary hydrides is stabilized by the presence of strong Li–H bonding. In these compounds, there is only one type of crystallographically distinct Li_6-octahedral H interstitial site. *Tt* atoms form long-range *Tt*-*Tt* chains sandwiched between Li-octahedra layers. From our DFT calculations, Li atoms transfer their electrons to both H and *Tt*. Li-H exhibits strong ionic bonding. *Tt* atoms accept electrons from Li and are covalently bonded with their neighbors within the *Tt*-*Tt* chains. The calculated total DOS indicates that both hydrides are metals. The observed vibrational spectra of these hydrides are in good overall agreement with the calculated phonon density of states. Splitting of the in-plane H vibrational peaks was observed, indicating dispersion of these lattice modes that can be ascribed to the coupling of H vibrations within the Li_6-octahedra layers.

ACKNOWLEDGMENTS

This work was partially supported by DOE through EERE Grant No. DE-AI-01-05EE11104 (H.W. and T.J.U.), EERE Grant No. DE-FC36-04GO14282 (W.Z.), BES Grant No. DE-FG02-98ER45701 (W.Z., T.Y.), and EERE Grant No. DE-AI-01-06EE11105 (R.C.B) and was partially performed at the Jet Propulsion Laboratory, California Institute of Technology, under a contract with the National Aeronautical and Space Administration.

*Author to whom correspondence should be addressed. huiwu@nist.gov

[1] C. van der Marel, G. J. B. Vinke, and W. van der Lugt, Solid State Commun. **54**, 917 (1985).

[2] R. A. Sharma and R. N. Seefurth, J. Electrochem. Soc. **123**, 1763 (1976).

[3] M. H. Braga, L. F. Malheiros, and I. Ansara, J. Phase Equilib. **16**, 324 (1995).

[4] L. A. Stearns, J. Gryko, J. Diefenbacher, G. K. Ramachandran, and P. F. McMillan, J. Solid State Chem. **173**, 251 (2003).
[5] R. C. Bowman, Jr., S.-J. Hwang, C. C. Ahn, and J. J. Vajo, Mater. Res. Soc. Symp. Proc. **837**, 3.6.1 (2005).
[6] J. J. Vajo, F. Mertens, C. C. Ahn, R. C. Bowman, Jr., and B. Fultz, J. Phys. Chem. B **108**, 13977 (2004).
[7] H. Wu, M. R. Hartman, T. J. Udovic, J. J. Rush, W. Zhou, R. C. Bowman, Jr., and J. J. Vajo, Acta Crystallogr., Sect. B: Struct. Sci. **63**, 63 (2007).
[8] S. Bobev and S. C. Sevov, J. Solid State Chem. **153**, 92 (2000).
[9] Certain commercial suppliers are identified in this paper to foster understanding. Such identification does not imply that the materials or equipment identified are necessarily the best available for the purpose.
[10] R. M. Lindstrom, J. Res. Natl. Inst. Stand. Technol. **98**, 127 (1993).
[11] T. J. Udovic, D. A. Neumann, J. Leão, and C. M. Brown, Nucl. Instrum. Methods Phys. Res. A **517**, 189 (2004).
[12] S. Baroni, A. Dal Corso, S. de Gironcoli, and P. Giannozzi, http://www.pwscf.org
[13] G. Kresse, J. Furthmuller, and J. Hafner, Europhys. Lett. **32**, 729 (1995).
[14] T. Yildirim, Chem. Phys. **261**, 205 (2000).
[15] U. Frank and W. Mueller, Z. Naturforsch. B **30**, 313 (1975).
[16] V. Hopf, H. Schaefer, and A. Weiss, Z. Naturforsch. B **25**, 653 (1970).
[17] U. Frank, W. Mueller, and H. Schaefer, Z. Naturforsch. B **30**, 10 (1975).
[18] H. G. von Schnering, R. Nesper, K. F. Tebbe, and J. Curda, Z. Metallkd. **71**, 357 (1980).
[19] R. Nesper, H. G. von Schnering, and J. Curda, Chem. Ber. **119**, 3576 (1986).
[20] G. L. Squires, *Introduction to the Theory of Thermal Neutron Scattering* (Dover, New York, 1996).